BIOELECTRICITY
Volume 1, Number 3, 2019

DOI: 10.1089/bioe.2019.0020

Ultrasensitive System for Electrophysiology of Cancer Cell Populations: A Review

Paulo R.F. Rocha, PhD,[1] Aya Elghajiji,[1,2] and David Tosh, PhD[1,2]

Abstract

Bioelectricity is the electrical activity produced by living organisms. Understanding the role of bioelectricity in a disease context is important as it contributes to both disease diagnosis and therapeutic intervention. Electrophysiology tools work well for neuronal cultures; however, they are limited in their ability to detect the electrical activity of non-neuronal cells, wherein the majority of cancers arise. Electronic structures capable of detecting and modulating signaling, in real-time, in electrically quiescent cells are urgently required. One of the limitations to understanding the role of bioelectricity in cancer is the inability to detect low-level signals. In this study, we review our latest advances in devising bidirectional transducers with large electrode areas and concomitant low impedances. The resulting high sensitivity is demonstrated by the extracellular detection of electrical activity in Rat-C6 glioma and prostate cancer (PC-3) cell populations. By using specific inhibitors, we further demonstrated that the large electrical activity in Rat-C6 glioma populations is acidosis driven. For PC-3 cells, the use of a calcium inhibitor together with the slowly varying nature of the signal suggests that Ca^{2+} channels are involved in the cohort electrogenicity.

Keywords: glioma, prostate cancer, ultrasensitive transducers, large area electrodes

Introduction

According to the Brain Tumor Charity, the World Health Organization and Cancer Research UK, brain tumors in children and adults <40 years and prostate cancer in men are among the most common malignant cancers occurring worldwide.[1,2] Cancer generally arises when transformed cells start to continually proliferate and spread in an unregulated manner, thus requiring an urgent need for early detection and efficient treatment to halt cancer development and metastasis. Although progress has been made in understanding the mechanisms underlying cancer development and progression, efficient therapeutic interventions are still lacking. One tool that could lead to potential breakthroughs in cancer research is electrophysiology. The problem is that only neuronal cells have classically been known to be electrogenic. This is partly because only neurons are recorded in conventional electrophysiology systems focusing on neuronal action potentials. Hence, there is still limited scientific understanding on the electrophysiology of the metastatic patterns of several forms of cancer, thus delaying the development of new targeted drugs for confinement and treatment of tumors.[3]

Defining the electrophysiological properties of both neuronal and non-neuronal cell types will directly benefit both disease detection and intervention. Membrane fluctuations caused by ion gradients play a key role within cells of the nervous system, and are caused by the flux of primarily Na^+, K^+, Cl^-, and Ca^{2+}, along with the gradients controlled by the activity of various ion channel protein families.[4,5] In neurons, depolarization of the membrane potential can lead to a substantial transient reversal of electric polarity of the cell membrane, known as the action potential.[4,6] Contrary to neuronal electrophysiology wherein the potential can reach >100 mV, electrophysiology of non-neuronal cells has been a technical challenge wherein signals may be orders of magnitude lower.

Non-neuronal cancer-derived cells such as the gold standard of prostate cancer cell culture line, PC-3 cells,[3,7] glial cells, as well glia-derived glioma, which retain among others, the expression of neurotransmitter receptors and voltage-gated ion channels, do not exhibit unbiased action potentials.[8,9]

[1]Centre for Biosensors, Bioelectronics and Biodevices (C3Bio), Department of Electronic and Electrical Engineering, University of Bath, Bath, United Kingdom.
[2]Centre for Regenerative Medicine, Department of Biology and Biochemistry, University of Bath, Bath, United Kingdom.

Instead, those known to be electrically quiescent cells exhibit distinctive single-cell oscillations of the membrane potential. Yet their excitability and membrane depolarization are considered to be functionally relevant, contributing to several functions including adjusting glia-mediated neurotransmitter uptake and discharge,[10] proliferation,[11,12] and oxidative stress.[13]

As the electrical activity of non-neuronal cells is minute and difficult to detect, we have derived ultrasensitive electrical transducers to enable electrophysiological recordings.[14,15] In this study, we review our recent advances in sensitive transducers to decode cancer cell–cell communication with emphasis on pH-sensitive rat C6 glioma cells[16,17] and human prostate cancer cell model PC-3.[7]

Ultrasensitive Transducers

The activity of electrogenic cells, specifically neurons, can be recorded, or stimulated, through several methodologies of different neural resolution ranging from intracellular, using patch or sharp electrodes, to microelectrode arrays (MEAs). These substrate-integrated MEAs permit a simultaneous noninvasive method of examining long-term recordings of extracellular local field potentials.[18,19]

Developed at the beginning of the 1970s, MEAs are typically composed of an array of electrodes that are either planar or three-dimensional, permitting close contact with cells in culture.[20–22] The electrodes are frequently made of gold (Au), platinum (Pt), titanium nitride, or alloys such as iridium oxide, with a diameter ranging between 10 and 100 μm, integrated into either a glass or a silicon wafer substrate.[6,23]

The MEA community pursues recording optimization by improving the electrical coupling between cell membrane and electrode by decreasing the electrode impedance. To improve the signal, the impedance should be as small as possible as compared with the amplifier input impedance. It is a challenge to achieve low impedance with micrometer-sized planar electrodes. Therefore, recent developments have focused on increasing the effective surface area by the utilization of biocompatible porous conducting materials such as Pt black, Au nanostructures, and carbon nanotubes.[6,23] By modifying the surface topology, the impedance of the electrode is reduced, cell attachment improved, leading to improved electrical recordings.[14,15]

We teemed our platform bidirectional because it allows electrical recordings of cell populations over time and under different pharmacological compounds. ''The sensor consists of a glass substrate on which circular electrodes of 100 nm Au on top of a 4 nm Cr adhesion layer were evaporated through a shadow mask. The surface roughness was measured with a DEKTAK—surface profilometer—and reached less than 1 nm. The area for C6 glioma recordings amounted to 10.5 mm^2.'' The electrode layout is optimized to gather long-term synchronized signals from a whole cell population adhered to the electrode. The sensors comprise two parallel circular electrodes, with one of them acting as the measuring electrode, whereas the other as a counterelectrode. The equivalent circuit (shown in Fig. 1a) embodies the electrical coupling between a population of cells and the electrode. This circuit has been recently explained in the literature.[14,15,17] In short, the equivalent model takes into account the electrical double layer established at a metal–electrolyte interface. The parallel circuit network is formed by the charge transfer resistance, R_D, and the Helmholtz–Gouy–Chapman double-layer capacitance, C_D, in series with the spreading resistance, R_C, that accounts for the signal loss into the surrounding electrolyte. A similar circuit describes the counter electrode. The electrical path from the sensing to the counter electrode has impedance, Z_{seal}. We then amplify the cell current fluctuations, $i(t)$. This current appears as a displacement current across the double-layer capacitance and is amplified by a transimpedance amplifier. The detected current, as originally demonstrated in Medeiros et al.,[14] is given as

$$\mathrm{i(t)} = \frac{\mathrm{dvs}}{\mathrm{dt}} \mathrm{C_D}\left(1 - \mathrm{e}^{-\frac{t}{\tau}}\right), \text{ with } \tau = \mathrm{R}_c\mathrm{R}_D. \qquad (1)$$

In this case, τ is the time constant for the charging or discharging of the network. C_D acts as a multiplying factor, which affects the spatial resolution, but also allows the amplification of the signal, thanks to the rescaling of C_D due to the use of large area electrodes. Changes in the extracellular potentials affect the current, which is the derivative of the acquired voltage signal.

To illustrate the importance of the electrode impedance for the background noise, we calculated the electrochemical noise as a function of electrode area, as depicted in Figure 2b. To achieve this, we model our electrode–electrolyte system as a double R_C (as depicted in Fig. 1a), where the electrode is characterized by a charge transfer resistance in parallel with a constant phase element representing the double layer capacitance. The R_C network is then in series with a spreading resistance representing the solution conductivity. The system has been explained in detail elsewhere.[15] With this analogy, we can more robustly model our electrode–electrolyte interface.[15]

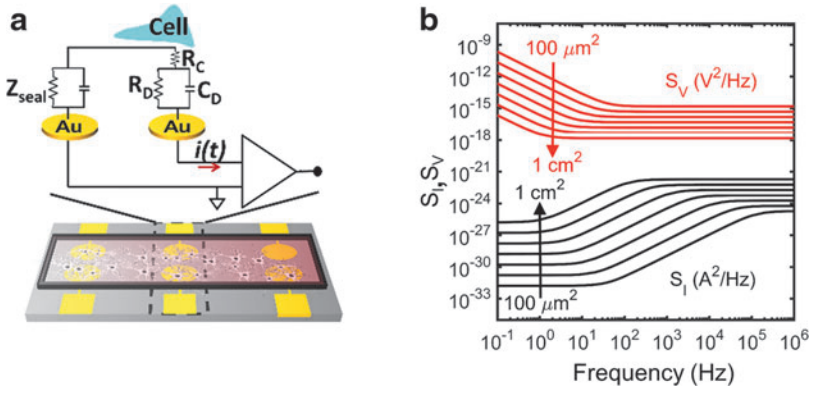

FIG. 1. Bidirectional transducer. **(a)** Sensor and equivalent circuit model for sensitive detection of adherent cells. **(b)** Calculated benchmark of current noise spectrum (S_I) in black and voltage noise spectrum (S_V) in red, for Au electrode–electrolyte interfaces as a function of electrode area varied by a factor of 10, from 100 μm^2 to 1 cm^2. The specific conductivity of the electrolyte was 200 Ωcm. Reproduced from Ref.[15] with permission from Scientific Reports. Au, gold.

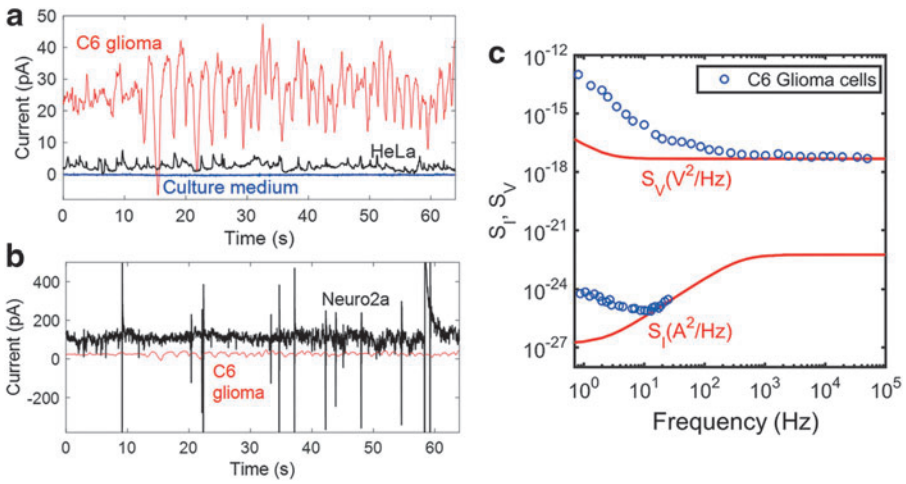

FIG. 2. **(a)** Time trace of the baseline with only C6 culture medium (blue), with HeLa cells (black) and with C6 glioma cells (red). Reproduced from Ref.[16] with permission from the Royal Society of Chemistry. **(b)** Time traces of neuroblastoma Neuro-2A cells (black) and C6 glioma cells (red). Reproduced from Ref.[16] with permission from the Royal Society of Chemistry. **(c)** The power spectral density of current noise, S_I, and voltage noise, S_V, as a function of frequency of a population of C6 glioma cells. The power spectral densities are averages of 20 consecutive unbiased measurements, of 60 s each. The electrode area was 10.5 mm^2. The solid lines are the calculated benchmark noise spectra of the bare Au electrodes in 100 mM aqueous KCl solution. Reproduced from Ref.[15] with permission from Springer Nature, Scientific Reports.

Figure 1b depicts the noise boundaries when using circular electrodes with areas varying from 100 μm^2 to 1 cm^2. Although the signal-to-noise ratio decreases with increasing frequency, at frequencies >10 Hz, the signal is controlled by the background noise of the electrode–electrolyte interface. At low frequency, the noise scales with the value of the charge transfer resistance. This means a linear increase of the current noise with electrode area, whereas concomitantly the voltage noise decreases with electrode area. Alternatively, at high frequencies, the charge transfer resistance is shunted by the double-layer capacitance and the impedance is dominated by the spreading resistance. The analysis indicates that the background noise increases with decreasing the charge transfer resistance. This means that to electrically detect sensitive electrical signals from cells, low impedance electrode interfaces are preferred. Hence, the most straightforward solution to optimize the impedance of the electrodes is to increase the electrode area.[17]

Thus, by minimizing the background noise through the use of low impedance large area electrodes and by minimizing external interferences using a set of Faraday's cages around the measurement equipment, we have shown that the noise level can be reduced from conventional 10–100 μVpp to only 0.3 μVpp.[15,16]

We note that the signals recorded using our large electrode area are the sum of all individual cell contributions. We estimate $\sim$25,000 cells adhered to a 10.5 mm^2 electrode. Individual cell signals cannot be resolved with sufficient spatial information. Uncorrelated cell activity appears as noise and low magnitude asynchronous spikes. Asynchronous current fluctuations of individual cells should largely cancel each other out, given the sufficiently high number of cells measured simultaneously. Instead, we propose that these current oscillations are either coordinated or occur simultaneously across a population of adherent cells.

Electrochemical Noise Analysis

To test the background noise level for the transducer, only cell culture medium was placed in the device (Fig. 2a, in blue). The current noise level revealed a small value of only 100 fA.[16] As a control experiment, we employed a human cervical carcinoma cell line HeLa, because these cells did not originate from the brain nor from any other electrically active tissue. Yet, owing to the high sensitivity of our system, we could even detect residual fluctuations of their basal current level (Fig. 2a, in black). Fluctuations near 3 pA were detected and differences between C6 and HeLa cells was reported.[16] C6 glioma cells were chosen as they were a robust and available model to validate the detection system. In fact, the current noise fluctuations of C6 glioma cells are comparatively larger than that of HeLa cells.

To prove the system's appropriateness for bioelectric detection, we first recorded the electric currents in neuronal populations, because they are broadly accepted as the most electroactive cells able to generate strong membrane depolarizations. We, therefore, as a benchmark used the murine neuroblastoma cell line Neuro-2A (N2A), which displays imposing electric excitability in a single-cell patch-clamp assay due to their neuronal origin.[5,9] We were able to show that N2A cell populations can easily be detected and are capable of distinctive electric firing reaching up to 400 pA of amplitude (Fig. 2a). These recordings were then compared with the glioma cell line C6 (Fig. 2b). As expected, we observed a much lower amplitude of signaling. By overlapping both HeLa and C6 cells, the measured currents are barely detectable when directly compared with that of the N2A cells (Fig. 2a). However, clearly the glioma cells exhibit electrical activity and are not electrically quiescent, as previous single-cell patch–clamp studies have suggested.[8,10]

Our methodology showed, for the first time, that recordings in glioma populations can be achieved when using external and highly sensitive electrodes rather than individually clamped cells.

For a more in-depth investigation, we analyzed the bioelectric activity in the frequency domain wherein the noise spectral density is presented on a double logarithmic scale as

a function of frequency. Figure 2c shows the current-noise and voltage-noise spectra of glioma cells. We have included the noise spectra of the bare electrodes in red. For clarity, we included the calculated noise spectra as they are similar to the recorded spectra. Below 10 Hz, the electrical activity of glioma can be clearly detected. Yet, at higher frequencies, the signals can no longer be distinguished from the background electrochemical noise of the electrode–electrolyte interface. Based on these results, we demonstrated that our sensing system allows noninvasive detection of extracellular field potentials of large cell populations over a wide range, from electrical bursts in the nanoampere range in neuronal cells (N2A) to miniscule basal current oscillations of electrically quiescent and nonexcitable cells (HeLa). Importantly, it allows the assessment of the spontaneous low-frequency electrical noise generated by populations of cancer cells.

Drug Screening Platform for Electroactive Cancers

After fabrication and characterization of devices capable of electrically detecting minuscule activity of cell–cell signaling, the source of the detected signal needs to be determined. Our bidirectional platform allows continuous electrical monitoring while exposing the cell population to pharmacological compounds. In addition, the analysis of biological signals has been performed using a highly sensitive method, in the frequency domain. In the same spectrum, one can retrieve information on calcium and sodium spikes and other switching behaviors between quiescent and bursting states,[17,24] in real time, and under different pharmacological compounds.

Voltage-gated Na^+ ion channels in electroactive glioma cells

The most aggressive and common form of primary adult brain tumor is malignant glioma. These are classified into three subcategories depending on the predominating glial cell type, astrocytoma, oligodendroglioma, and ependymoma.[25] The current standard treatment regimens include surgery, immunotherapy, chemotherapy, and radiotherapy, with most cases requiring a multidisciplinary approach, which have been proven inefficient in providing a better quality of life as well as long-term survival.[26–29]

The clinical presentation of glioma varies depending on the location of the tumor and the anatomic structure involved. Common presenting symptoms include increased intracranial pressure, in the form of persistent headaches, progressive neurofunctional deficits, and seizures. Around 25% of high-grade and 95% of low-grade glioma patients suffer from epileptic seizures, a high risk factor for long-term disability.[30–32] Current antiepileptic drugs are unable to circumvent the occurrence of ~50% of minor seizures and 5% of major seizures. Optimal clinical management of seizures associated with tumors is complicated by a lack of understanding of the mechanisms of seizure initiation. Complete seizure control cannot currently be achieved in all brain tumor patients.[33]

Voltage-gated Na^+ ion channels are the elementary channels for neuronal depolarization, which are vital for the resting potential and the propagation and/or generation of action potentials in neurons and often studied during epileptic events in glioma patients.[34] Voltage-gated Na^+ ion channels have been widely associated in enhancing the invasiveness of several forms of cancer, including glioma.[34–36] Thus, we examined the role of voltage-gated Na^+ ion channels in the generation of electric signaling in glioma cells. To this end, tetrodotoxin (TTX) is known to specifically inhibit the voltage-gated Na^+ channel without imposing on the functionality of other various types of Na^+ channels present in glia cells.[37] We investigated the effect of adding 1 μM of TTX to a population of freshly deposited adherent C6 glioma cells (Fig. 3a).

The analysis depicted in Figure 3a is in the frequency domain. The current noise spectra <10 Hz show a strong frequency dispersion and, therefore, cannot easily be ascribed to thermal adhesion noise. After adding TTX, the current noise spectrum, S_I, at 0.1 Hz decreases by two orders of

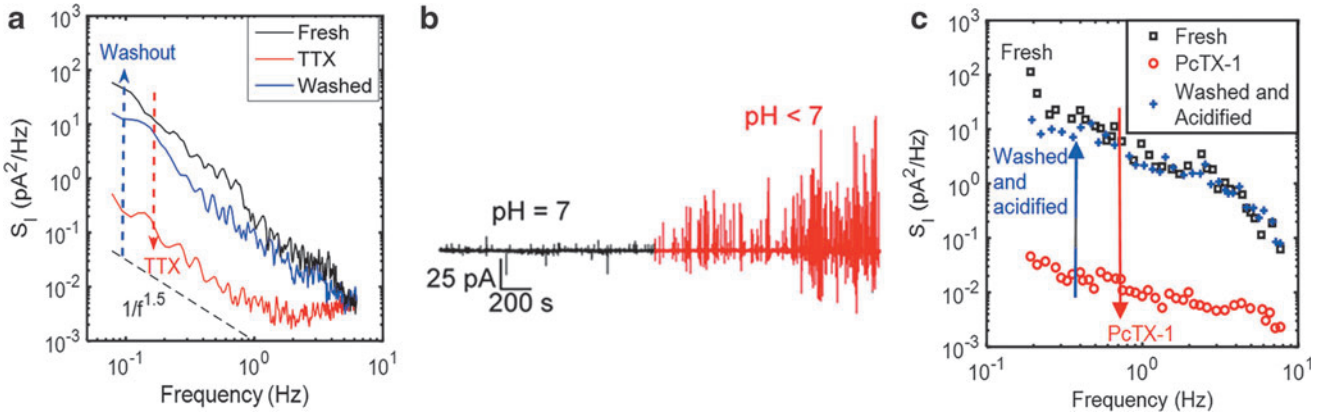

FIG. 3. Electrical signaling of glioma cells. **(a)** The current noise spectrum of fresh C6 glioma cells is represented in black. In red, the current noise spectrum is illustrated after adding 1 μM of TTX for 50 min. The blue trace represents the current noise spectrum after the inhibitor washout process. Measurement was taken 90 min after inhibitor washout. The dashed black curve in the bottom is a guide to the eye representing the proportionality of $1/f^{1.5}$ suggesting residual activity of other channels within the measured cells. Reproduced from Ref.[16] with permission from the Royal Society of Chemistry. **(b)** Time evolution of the current noise of C6 glioma cells. **(c)** Current noise spectra of C6 glioma cells upon adding PcTX-1, up to a concentration of 100 nM in acidified cell culture medium. The black line represents the original state. The red line is recorded after adding PcTX-1 to a concentration of only 100 nM. The blue curve represents the recovery plot after washing thrice. Reproduced from Ref.[17] with permission from Science Advances. PcTX-1, psalmotoxin-1; TTX, tetrodotoxin.

magnitude, within 25 min (Fig. 3a, solid red curve). At higher frequencies, between 1 and 10 Hz, the spectrum is flat as a result of adding 1 μM TTX. This means that thermal noise is observed at this frequency interval. Furthermore, the noise spectrum S_I follows a $1/f^{1.5}$ power law due to some residual activity between 60 mHz and 1 Hz, suggesting that we are not disrupting the functionality of other channels within the measured cells. After the washout process, the signal returns to its original form within 90 min (Fig. 3a, solid blue line). In addition, the thermal contribution of the cell noise vanishes as the original S_I becomes re-established.[16]

We concluded that freshly adhered C6 glioma cells produced a basal current noise of a few picoampheres and this residual activity was influenced by the flow of Na^+ ions through their respective voltage-gated channels.[16]

Role of acid sensing ion channels in electroactive glioma cells

We observed that when cells remain incubated for a period longer than 10 h, the current recordings unexpectedly transformed (Fig. 3b, in red). Whereas in the first hours of recordings the glioma electrical recordings reveal sporadic and weak patterns that evolve with time to a more active pattern characterized by an increase of both the firing rate and the spikes' magnitude rising from a few pA to $\sim$100 pA.[17]

We detected a prompt medium acidification over time. The pH dropped $\sim$1 U after 20 h.[17] We note that the increasing electrical activity in the recorded glioma populations is related to the decreased extracellular pH. To ascertain whether the emerging large electrical activity is pH triggered, we recorded the electrical activity of C6 cells upon addition of the highly specific inhibitor of acid sensing ion channels (ASICs), psalmotoxin (PcTx-1).[38] In acidified cells, the electric response exhibited large current spikes (Fig. 3c, black trace). Immediately after adding PcTX-1 to the cell medium up to a concentration of 100 nM, the large electrical activity stopped and recordings only showed basal current fluctuations (Fig. 4c, red curve). The cell medium was then washed to remove the PcTX-1 and left to acidify for $\sim$8 h. The acidified response re-established (Fig. 3c, blue trace).

We demonstrated that the increase in electrical activity is not related to apoptosis since the cells are viable and proliferative when the electrical activity is recorded.[17] With their disordered vasculature and rapid growth, tumors exhibit a strongly acidic extracellular environment due to the production of lactic acid.[39] By using specific inhibitors, we demonstrated that the large electrical activity in our glioma populations is stimulated by extracellular pH change that enhances Na^+ ion flux through the PcTX-1–sensitive ASICs.[17]

The discovery that the tumor itself is electrogenic and independent of any neuronal stimuli could be relevant for understanding the tumor's impact on brain electrophysiology, namely seizure initiation in glioma patients, once the pH measured in human brain tumors can reach as low as 5.9, as opposite to normal brain tissue with a pH value of $\sim$7.1.

Role of putative Ca^{2+} channels in electroactive prostate cancer cells

Prostate cancer is one of the most common malignancy cancers in men.[40,41] Currently, diagnosis is a significant challenge and, therefore, there is an urgent need for early prevention and efficient treatment. Yet, there is still minute scientific knowledge on the electrophysiology of the prostate cancer growth and metastatic patterns, therefore, postponing the development of new targeted drugs for confinement and treatment of the tumor.[3]

Reliable *in vitro* models for prostate cancer are LNCaP, DU-145, and PC-3 cells.[42,43] By applying a population of PC-3 cells to our sensors, we could, for the first time, detect their electrical signaling. In fact, two typical patterns were recorded: a weak and asynchronous pattern and a quasi-periodic pattern. The weak activity was characterized by asynchronous and sporadic spike amplitudes of $\sim$100 pA and widths between 30 and 200 ms. The origin is likely to relate with the known expression of K^+ channels of the Kv1.3 family and voltage-activated Na^+ currents as shown recently in prostate cancer cell lines through patch clamp experiments.[44–47]

The quasi-periodic spikes, however, were mostly characterized by larger signal magnitudes, with lower widths ranging from 0.03 to 0.3 s and the distance between spikes reaching a peak $\sim$2 to 3 s although the variation expands from 1 to 10 s of interval between biphasic spikes.[7] The spikes are larger and wider during the quasi-periodic activity, as expected for cooperative intracellular traveling waves.[15,17]

We observed that the quasi-periodic nature of signals is slow and routinely occurs during prostate cancer proliferation. In addition, the quasi-periodicity and form of the current signal match with an intracellular traveling wave across the

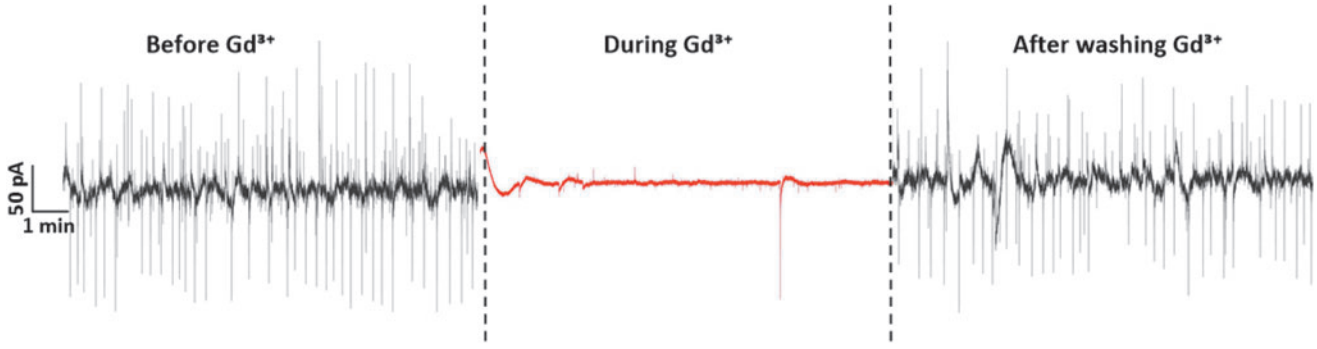

FIG. 4. Electrical activity of PC-3 cells culture before, during, and after using Gd^{3+} has been used as a Ca^{2+} inhibitor. Before and after the use of Gd^{3+}, the electrical activity shows quasi-periodic current oscillations. Reproduced from Ref.[7] with permission from MDPI Sensors.

electrode. Once the wave reaches the sensing electrode, it increases its potential relative to the counter electrode, forcing a large displacement current through the double-layer capacitance, originating the upward and downward current spikes, which corresponds to the wave entering and leaving the recording electrode.[14,15] We measured the time between upward and downward spikes to vary between 0.7 and 2 s, using 1 mm^2 electrodes. In other words, our recordings allow the monitoring of a traveling wave at a velocity of a few hundreds of micrometers per second, in agreement with Ca^{2+} wave speeds recorded in the literature.[11,12,48] In addition, previous imaging and single-cell studies investigated K^+, Na^+, and Ca^{2+} channels in human prostate cancer basal activity and proliferation.[49,50] Consensus on the role of Ca^{2+} channels during prostate cancer proliferation seems to exist as demonstrated by Zhang and colleagues through the use of Ca^{2+}-permeable channel TRPM8[13,51] and by others through a permeable channel to Ca^{2+}, TRPC6, and other oxidative stresses.[52]

We assumed that Ca^{2+} channels are involved due to their reported periodicity, kinetics, and contribution during PC-3 proliferation. However, to demonstrate a possible role of Ca^{2+} in the recorded electrical activity, we blocked the electrical spikes using a generic Ca^{2+} channel inhibitor, gadolinium (Gd^{3+}).[53–56]

First, we recorded the regular quasi-periodic activity of PC-3 cells (Fig. 4). Gd^{3+}, a Ca^{2+} inhibitor, was then added to the culture. The inhibitor at concentrations of 20 μM remained for 20 min before being washed out. Recordings were continuously made. The inhibitor effect is rapid and in <1 min, the current fluctuations were lowered to <5 pA of magnitude (Fig. 4, red trace). The cells were then washed three times with phosphate buffered saline to remove the Gd^{3+} inhibitor and fresh medium was provided. After washing out, the PC-3 cells regained the original electrical activity, yielding spike magnitudes of $\sim$100 pA as illustrated in the right ended black trace of Figure 4. Importantly, several controls have been made to ascertain that $GdCl_3$ is nontoxic to PC-3 cells during the experiments.[7]

Our recent results reveal that one of the most common malignant cancers diagnosed in men can also be electrically monitored in real time and employed into our drug-screening platform. This could be quite advantageous as still little scientific understanding on the electrophysiology of prostate cancer growth and metastatic patterns exists. This lack of knowledge is delaying the development of new targeted drugs for the confinement and treatment of this tumor.[3]

Conclusions

Minimally invasive electrophysiology coupled with processing tools such as electrical noise analysis holds great promise for novel therapeutic targets for cancer progression, particularly for predicting and preventing future metastatic development.

Our transducer comprises large electrode area with concomitant low impedance. Because low electrode impedance decreases the electrochemical background noise, the noise floor of our transducer can be one order of magnitude lower than state-of-the-art transducers, 0.3 μVpp, by using electrode areas up to a few square millimeters. The large area electrode allows the recording of whole cell populations instead of single cells. We, therefore, suggest this method for the investigation of whole cell populations that engage in cohort activity such as cancer cells.

The resulting high sensitivity is demonstrated by the extracellular detection of two of the most severe cancers, glioma and prostate cancers. The minute electrical activity could be detected below a frequency of $\sim$10 Hz in highly viable and proliferating cancer cell populations.

For glioma, the role that glial cells play in seizure onset is still unknown and all pieces of evidence suggest that they are as important as neurons. By using specific inhibitors, we demonstrated that the large electrical activity in rat C6 glioma populations is stimulated by extracellular pH changes that enhance Na^+ ion flux through the PcTX-1–sensitive ASICs. Hence, efforts toward the understanding of seizure development and improvement of seizure control for patients with glioma must be addressed while accounting for all electrogenic cells in the brain.

For PC-3 cells, the use of the calcium inhibitor Gd^{3+} together with the slowly varying nature of the signal suggests that Ca^{2+} channels are involved in the electrical signaling among a population of PC-3 cells during proliferation. This opens the door to more investigations to better understand the signaling pathways among prostate cancer cells at different tumor stages.

Acknowledgment

We thank Prof. Dago De Leeuw for reading this article.

Authors' Contributions

All coauthors wrote, reviewed, and approved the article before submission. This review article has been submitted solely to this journal.

Author Disclosure Statement

No competing financial interests exist.

Funding Information

No funding was received for this study.

References

1. The Brain Tumour Charity. 2019 Statistics about Brain Tumour. www.thebraintumourcharity.org/get-involved/donate/why-choose-us/the-statistics-about-brain-tumours/ (last accessed July 10, 2019).
2. Cancer Research UK. 2016 Statistics about Prostate Cancer. www.cancerresearchuk.org/health-professional/cancer-statistics/statistics-by-cancer-type/prostate-cancer (last accessed July 10, 2019).
3. Dozmorov MG, Hurst RE, Culkin DJ, et al. Unique patterns of molecular profiling between human prostate cancer LNCaP and PC-3 cells. Prostate 2009;69:1077–1090.
4. Hodgkin AL, Huxley AF. A quantitative description of membrane current and its application to conduction and excitation in nerve. J Physiol 1952;117:500–544.
5. Leung Y-M, Wu B-T, Chen Y-C, et al. Diphenidol inhibited sodium currents and produced spinal anesthesia. Neuropharmacology 2010;58:1147–1152.

6. Verkhratsky A, Krishtal OA, Petersen OH. From Galvani to patch clamp: The development of electrophysiology. Pflug Arch Eur J Phy 2006;453:233–247.
7. Cabello M, Ge H, Aracil C, et al. Extracellular electrophysiology in the prostate cancer cell model PC-3. Sensors (Basel, Switzerland) 2019;19:139.
8. Brismar T. Physiology of transformed glial cells. Glia 1995;15:231–243.
9. Brohawn SG, Su Z, MacKinnon R. Mechanosensitivity is mediated directly by the lipid membrane in TRAAK and TREK1 K^+ channels. Proc Natl Acad Sci USA 2014;111: 3614–3619.
10. Ordaz B, Vaca L, Franco R, et al. Volume changes and whole cell membrane currents activated during gradual osmolarity decrease in C6 glioma cells: Contribution of two types of K+ channels. Am J Physiol Cell Physiol 2004;286: C1399–C1409.
11. Leybaert L, Sanderson MJ. Intercellular Ca(2+) waves: mechanisms and function. Physiol Rev 2012;92:1359–1392.
12. Charles AC, Naus CC, Zhu D, et al. Intercellular calcium signaling via gap junctions in glioma cells. J Cell Biol 1992;118:195–201.
13. Gkika D, Flourakis M, Lemonnier L, et al. PSA reduces prostate cancer cell motility by stimulating TRPM8 activity and plasma membrane expression. Oncogene 2010; 29:4611.
14. Medeiros MCR, Mestre A, Inácio P, et al. An electrical method to measure low-frequency collective and synchronized cell activity using extracellular electrodes. Sensing Biosensing Res 2016;10:1–8.
15. Rocha PRF, Schlett P, Kintzel U, et al. Electrochemical noise and impedance of Au electrode/electrolyte interfaces enabling extracellular detection of glioma cell populations. Sci Rep 2016;6:34843.
16. Rocha PRF, Schlett P, Schneider L, et al. Low frequency electric current noise in glioma cell populations. J Mater Chem B 2015;3:5035–5039.
17. Rocha PRF, Medeiros MCR, Kintzel U, et al. Extracellular electrical recording of pH-triggered bursts in C6 glioma cell populations. Sci Adv 2016;2:e1600516.
18. Pine J. Recording action potentials from cultured neurons with extracellular microcircuit electrodes. J Neurosci Methods 1980;2:19–31.
19. Baumann WH, Lehmann M, Schwinde A, et al. Microelectronic sensor system for microphysiological application on living cells. Sensor Actuat B Chem 1999;55:77–89.
20. Hoogerwerf AC, Wise KD. A three-dimensional microelectrode array for chronic neural recording. IEEE Trans Biomed Eng 1994;41:1136–1146.
21. Thiebaud P, deRooij NF, KoudelkaHep M, et al. Microelectrode arrays for electrophysiological monitoring of hippocampal organotypic slice cultures. IEEE T Biomed Eng 1997;44:1159–1163.
22. Ferrea E, Maccione A, Medrihan L, et al. Large-scale, high-resolution electrophysiological imaging of field potentials in brain slices with microelectronic multielectrode arrays. Front Neural Circuits 2012;6:80.
23. Buzsáki G, Anastassiou CA, Koch C. The origin of extracellular fields and currents—EEG, ECoG, LFP and spikes. Nat Rev Neurosci 2012;13:407.
24. Abbasi S, Abbasi A, Sarbaz Y, et al. Power spectral density analysis of purkinje cell tonic and burst firing patterns from a rat model of ataxia and riluzole treated. Basic Clin Neurosci 2017;8:61–68.
25. Louis DN, Perry A, Reifenberger G, et al. The 2016 World Health Organization classification of tumors of the central nervous system: A summary. Acta Neuropathol 2016;131: 803–820.
26. Stupp R, Mason WP, van den Bent MJ, et al. Radiotherapy plus concomitant and adjuvant temozolomide for glioblastoma. N Engl J Med 2005;352:987–996.
27. Furnari FB, Fenton T, Bachoo RM, et al. Malignant astrocytic glioma: Genetics, biology, and paths to treatment. Genes Dev 2007;21:2683–2710.
28. Komotar RJ, Otten ML, Moise G, et al. Radiotherapy plus concomitant and adjuvant temozolomide for glioblastoma-a critical review. Clin Med Oncol 2008;2:421–422.
29. Minniti G, Lanzetta G, Scaringi C, et al. Phase II study of short-course radiotherapy plus concomitant and adjuvant temozolomide in elderly patients with glioblastoma. Int J Radiat Oncol Biol Phys 2012;83:93–99.
30. Lacroix M, Abi-Said D, Fourney DR, et al. A multivariate analysis of 416 patients with glioblastoma multiforme: Prognosis, extent of resection, and survival. J Neurosurg 2001;95:190–198.
31. Wen PY, Marks PW. Medical management of patients with brain tumors. Curr Opin Oncol 2002;14:299–307.
32. Pruitt AA. Medical management of patients with brain tumors. Curr Treat Option Ne 2011;13:413–426.
33. Epilepsy Society. 2018 Statistics about Epilepsy. www .epilepsysociety.org.uk/facts-and-statistics#.XXgbrij0kdU (last accessed July 10, 2019).
34. Molenaar RJ. Ion channels in glioblastoma. ISRN Neurol 2011;2011:590249.
35. Joshi AD, Parsons DW, Velculescu VE, et al. Sodium ion channel mutations in glioblastoma patients correlate with shorter survival. Mol Cancer 2011;10:17.
36. Pollak J, Rai KG, Funk CC, et al. Ion channel expression patterns in glioblastoma stem cells with functional and therapeutic implications for malignancy. PLoS One 2017; 12:e0172884.
37. Lee CH, Ruben PC. Interaction between voltage-gated sodium channels and the neurotoxin, tetrodotoxin. Channels 2008;2:407–412.
38. Escoubas P, De Weille JR, Lecoq A, et al. Isolation of a tarantula toxin specific for a class of proton-gated Na+ channels. J Biol Chem 2000;275:25116–25121.
39. Swietach P, Hulikova A, Vaughan-Jones RD, et al. New insights into the physiological role of carbonic anhydrase IX in tumour pH regulation. Oncogene 2010;29:6509–6521.
40. NCISCS. SEER Cancer Statistics Review (CSR) 1975–2015. https://seer.cancer.gov/csr/1975_2015 (last accessed April 18, 2018).
41. Weiner AB, Matulewicz RS, Eggener SE, et al. Increasing incidence of metastatic prostate cancer in the United States (2004–2013). Prostate Cancer Prostatic Dis 2016;19:395.
42. Stone KR, Mickey DD, Wunderli H, et al. Isolation of a human prostate carcinoma cell line (DU 145). Int J Cancer 1978;21:274–281.
43. Cunningham D, You Z. In vitro and in vivo model systems used in prostate cancer research. J Biol Methods 2015;2: pii: e17.
44. Teulon J, Ronco PM, Geniteau-Legendre M, et al. Transformation of renal tubule epithelial cells by simian virus-40 is associated with emergence of Ca2+-insensitive K+ channels and altered mitogenic sensitivity to K+ channel blockers. J Cell Physiol 1992;151:113–125.

45. Ouadid-Ahidouch H, Van Coppenolle F, Le Bourhis X, et al. Potassium channels in rat prostate epithelial cells. FEBS Lett 1999;459:15–21.
46. Djamgoz MBA, Mycielska M, Madeja Z, et al. Directional movement of rat prostate cancer cells in direct-current electric field. J Cell Sci 2001;114:2697.
47. Laniado ME, Lalani EN, Fraser SP, et al. Expression and functional analysis of voltage-activated Na+ channels in human prostate cancer cell lines and their contribution to invasion in vitro. Am J Pathol 1997;150:1213–1221.
48. Boitano S, Dirksen ER, Sanderson MJ. Intercellular propagation of calcium waves mediated by inositol trisphosphate. Science (New York, NY) 1992;258:292–295.
49. Abdul M, Hoosein N. Expression and activity of potassium ion channels in human prostate cancer. Cancer Lett 2002; 186:99–105.
50. Yildirim S, Altun S, Gumushan H, et al. Voltage-gated sodium channel activity promotes prostate cancer metastasis in vivo. Cancer Lett 2012;323:58–61.
51. Zhang L, Barritt GJ. Evidence that TRPM8 is an androgen-dependent $Ca2^{+}$ channel required for the survival of prostate cancer cells. Cancer Res 2004;64:8365–8373.
52. Holzmann C, Kilch T, Kappel S, et al. Differential Redox regulation of Ca2+ signaling and viability in normal and malignant prostate cells. Biophys J 2015;109:1410–1419.
53. Boland LM, Brown TA, Dingledine R. Gadolinium block of calcium channels: Influence of bicarbonate. Brain Res 1991;563:142–150.
54. Bourne GW, Trifaró JM. The gadolinium ion: A potent blocker of calcium channels and catecholamine release from cultured chromaffin cells. Neuroscience 1982;7: 1615–1622.
55. Guilak F, Zell RA, Erickson GR, et al. Mechanically induced calcium waves in articular chondrocytes are inhibited by gadolinium and amiloride. J Orthop Res 1999;17:421–429.
56. Lacampagne A, Gannier F, Argibay J, et al. The stretch-activated ion channel blocker gadolinium also blocks L-type calcium channels in isolated ventricular myocytes of the guinea-pig. Biochim Biophys Acta 1994;1191:205–208.

Address correspondence to:
Paulo R.F. Rocha, PhD
Centre for Biosensors, Bioelectronics and Biodevices (C3Bio)
Department of Electronic and Electrical Engineering
University of Bath
Claverton Down
Bath BA2 7AY
United Kingdom

E-mail: p.rocha@bath.ac.uk